Electronic Supplementary Information

New phenazine based anolyte material for high voltage organic redox flow batteries

Elena I. Romadina [a,b,*], Denis S. Komarov [a,c], Keith J. Stevenson [a], and Pavel A. Troshin [b]

[a.] *Center for Energy Science and Technology, Skolkovo Institute of Science and Technology, Bolshoy Boulevard 30, bld.1, Moscow, 143026, Russian Federation*

[b.] *Institute of Problems of Chemical Physics, Russian Academy of Sciences, Semenov Prospect 1, Chernogolovka, Moscow region, 142432, Russian Federation*

[c.] *D. Mendeleev University of Chemical Technology of Russia, Miusskaya ploshchad' 9, Moscow, 125047, Russian Federation*

**E-mail address: Elena.Romadina@skoltech.ru*

1. Experimental methods

Materials, purification and characterisation techniques: All solvents and reagents were purchased from Sigma-Aldrich or Acros Organics and used as received or purified according to standard procedures. Acetonitrile for the RFB experiments was additionally dried over 4Å molecular sieves in Ar glovebox. The target compound was purified using a preparative Shodex GPC column (20 mm × 300 mm, 1 mL min^{-1}) and toluene as eluent. Purity of the synthesized components was controlled by high performance liquid chromatography on Shimadzu-20A instrument with the use of C_{18} analytical column.

NMR measurements: The ^{1}H and ^{13}C NMR spectra were obtained using Bruker AVANCE III 500 instrument. Chemical shifts are referenced to the residual solvent signals: 7.28 ppm for ^{1}H and 77.16 ppm for ^{13}C in $CDCl_3$.

Thermal gravimetry analysis: Thermal stability of **M1** was investigated using TGA-2 thermogravimetric analyzer (Mettler Toledo) at a heating rate of 10°C min^{-1} and a N_2 flow of 20 ml min^{-1}. The mass of the sample was ~4 mg.

Solubility test: The acetonitrile or acetonitrile solution of 5M $TBABF_4$ was added drop by drop to 81.0 mg (0.2 mmol) of **M1** powders and rigorously mixed at the room temperature, until the powders were fully dissolved. The weights of added solvent and obtained solution were measured for the calculation of **M1** concentration.

Membrane preparation: Neosepta AHA anion exchange membrane was obtained from Astom corp. Membrane was prepared for using standard procedure: membrane was conditioned in acetonitrile-water (50:50) solvents mixture for 1h at 60˚C, in pure MeCN at 60˚C for 1 h and in 0.05 M supporting electrolyte solution in MeCN for 24-hour period under the room temperature and ambient conditions.

Electrochemical tests: Cycling voltammograms were recorded in three-electrode cell with glassy carbon working electrode (WE) (d = 5 mm) (for the Scan-rate-dependent CV measurements WE with d = 3 mm was applied), $Ag/AgNO_3$ reference electrode (RE) (Basi, 10 mM $AgNO_3$ in MeCN) calibrated by ferrocene and Pt wire counter electrode (CE). Ferrocene peak was determined as -0.01 V vs. $Ag/AgNO_3$. Before the experiments, argon was purged through the electrolyte for 15 minutes. WE was preliminary polished with ¼ μm diamond suspension. Concentration of the active substances was 3 mM in 0.1 M background $TBABF_4$ electrolyte based on anhydrous MeCN. CV tests measurements were performed on Metrohm Autolab potentiostate.

Flow cell tests: A redox flow cell which was used for the experiments is presented in Figure S1. Electrodes were cut from 6 mm thick graphite felt, and put into the assembled flow cell, providing a geometric active area of 4.00 cm^2. Anion-exchange Neosepta AHA membrane was used as the separator. Teflon gaskets sealed the membrane and electrodes into the cells. Flow cells were assembled inside the glovebox with both H_2O and O_2 levels below 1 ppm. Peristaltic pump Heildolf Hei-Flow Precision 0.1 Multi was used to drive redox electrolytes from the reservoirs to the flow cell with the 10 mL min^{-1} flow rate.

In order to neglect crossover-induced capacity fade, 10 mL of mixed electrolytes with 10 mM concentration of active substances and 0.1 M of supporting electrolyte ($TBABF_4$) in anhydrous MeCN were used. Combined galvanostatic and potentiostatic cycling regime was performed using Ellins potentiostate (Electrochemical instruments, Russia). Cell was charged at 2 mA current till upper cutoff, then discharged at the same current; after reaching the lower cutoff, the potential was held for 2000 seconds in order to provide deeper discharge of the battery. The theoretical capacity of the battery calculated as 268 mA h L^{-1}.

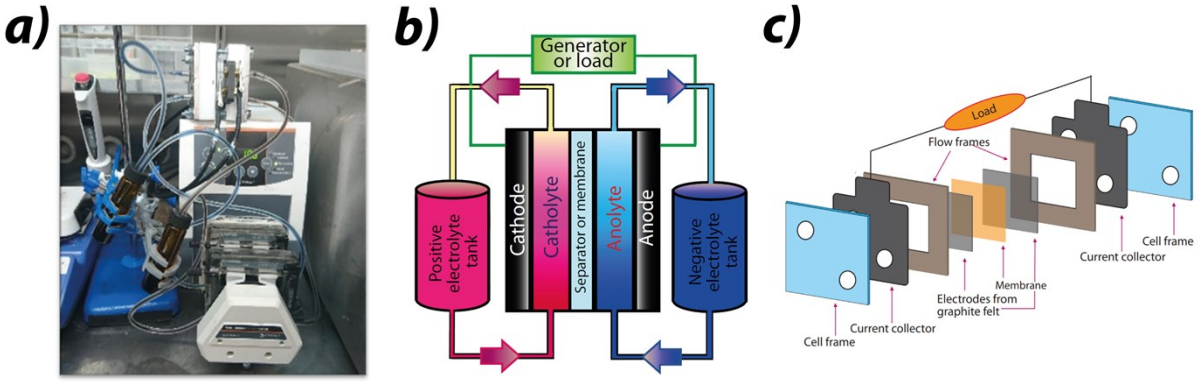

Figure S1. (a) Photo of a homemade redox flow cell (b) Schematic view of a redox flow battery system (c) Schematic diagram of the laboratory RFB cell composed of ion-exchange membrane (Neosepta AHA), electrodes from the graphite felt, graphite/Teflon current collectors, Teflon flow frames, and metal cell frames.

Flow cell resistance measurements: Impedance curves were recorded on Metrohm Autolab potentiostat. For the measurements, the described above flow cell was used.

2. Synthesis

2-[2-(2-Methoxyethoxy)ethoxy]ethyl}-4-methylbenzene-sulfonate

2-[2-(2-Methoxyethoxy)ethoxy]ethyl}-4-methylbenzene-sulfonate was synthesized according to previously reported procedure [1].

*Compound (**2**) phenazine-2,3-diol*

Compound (**2**) was prepared following the procedure described by C. Seillan et. al. [2]. A mixture of *o*-diaminobenzene (2.00 g, 18.49 mmol, 1 equiv) and 2,5-dihydroxy-*p*-benzoquinone (2.85 g, 20.34 mmol, 1.1 eq.) in 10 ml of deionized water was heated at reflux for 1 h. The obtained dark-red precipitate was isolated by filtration, washed with 20 ml of distilled water affording 2.18 g of compound (**2**) with 55 % yield.

^{1}H NMR (400 MHz; DMSO-d^6) = 10.94 (br s, 2H), 8.03 (br s, 2H), 7.71 (br s, 2H), 7.27 (br s, 2H)

*Compound 2,3-bis(2-(2-methoxyethoxy)ethoxy)phenazine (**M1**)*

The synthesis of **M1** was performed following a general procedure of J. Winsberg [3]. Mixture of phenazine-2,3-diol (1.00 g, 4.71 mmol, 1.0 equiv), 2-[2-(2-methoxyethoxy)ethoxy]ethyl]-4-methylbenzene-sulfonate (2.97 mg, 10.87 mmol, 2.3 equiv),

K_2CO_3 (3.25 mg, 23.55 mmol, 5.0 equiv) and 30 ml of anhydrous DMF was stirred at 80˚C under the argon atmosphere for 15h. The DMF was removed in vacuum, the product was extracted from the residue by CH_2Cl_2, washed with ice water (30 mL), then the organic phase was isolated, dried over Na_2SO_4 and concentrated under reduced pressure. The 1.68 g of pure product was obtained after the GPC purification with 87% yield.

^{1}H NMR (400 MHz; $CDCl_3$): δ (ppm) 8.09 (m, 2H), 7.69 (m, 2H), 7.31 (m, 2H), 4.33 (t, 4H), 3.96 (t, 4H), 3.75 (m, 4H), 3.54 (m, 4H), 3.35 (s, 6H).

^{13}C NMR (126 MHz; $CDCl_3$): 154.06, 141.68, 141.66, 129.14, 128.69, 105.80, 72.02, 71.02, 69.16, 68.84, 59.08.

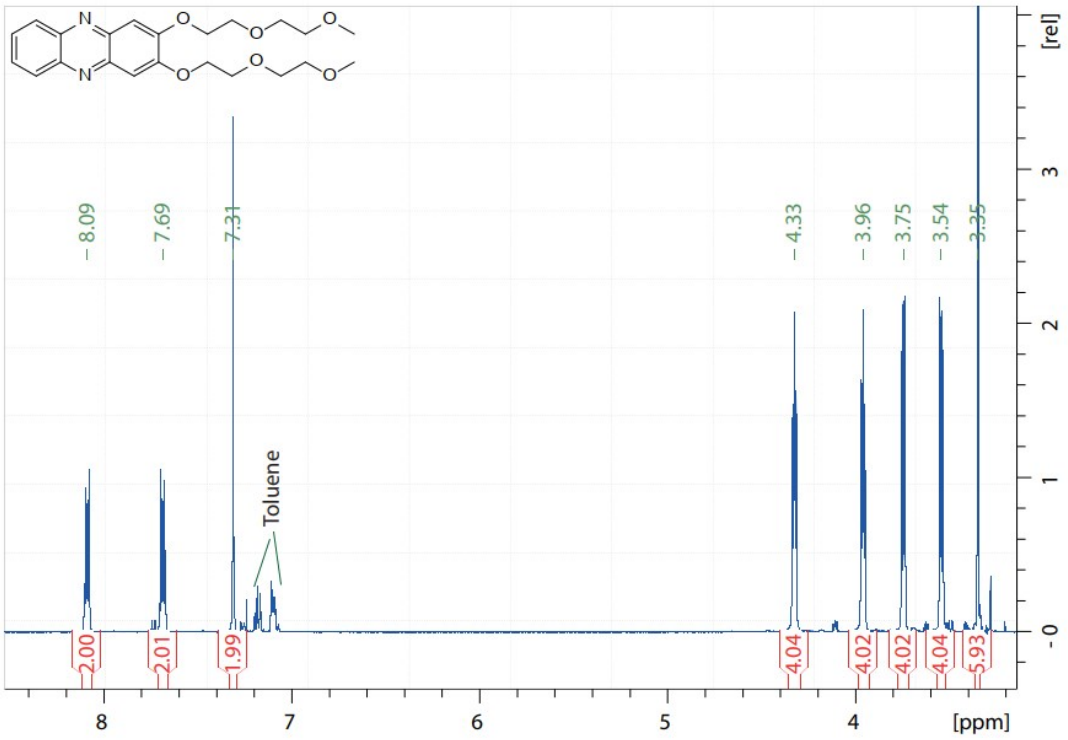

Figure S2. ^{1}H NMR spectrum of 2,3-bis(2-(2-methoxyethoxy)ethoxy)phenazine

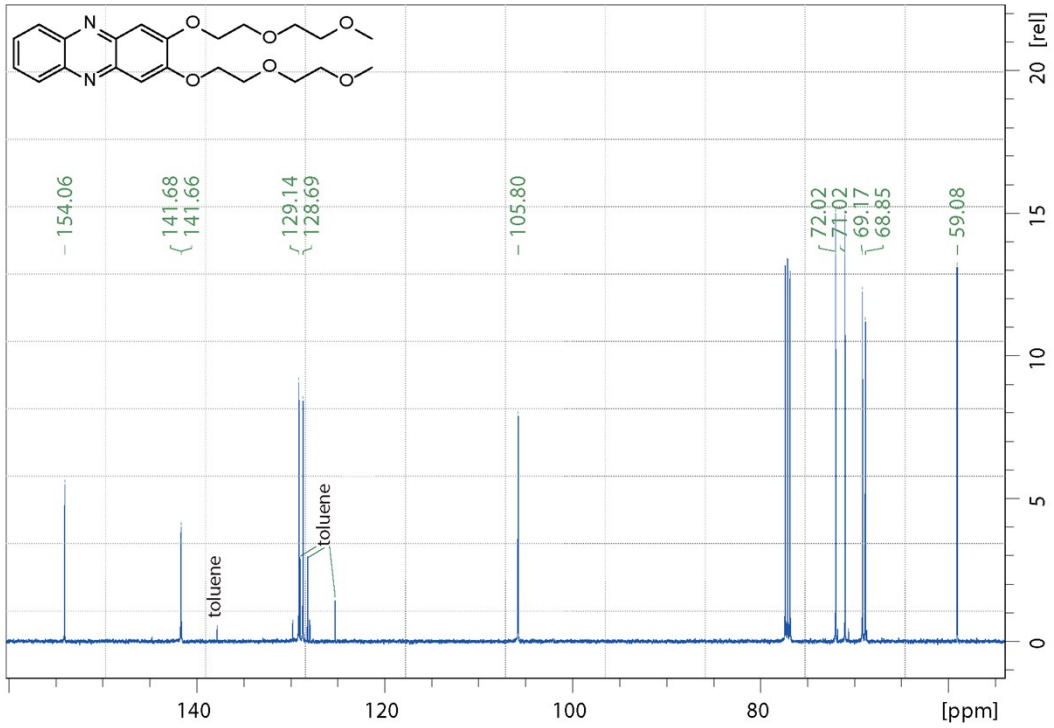

Figure S3. ^{13}C NMR spectrum of 2,3-bis(2-(2-methoxyethoxy)ethoxy)phenazine

*Compound (**M2**) 2,3-bis(2-(2-methoxyethoxy)ethoxy)phenazine*

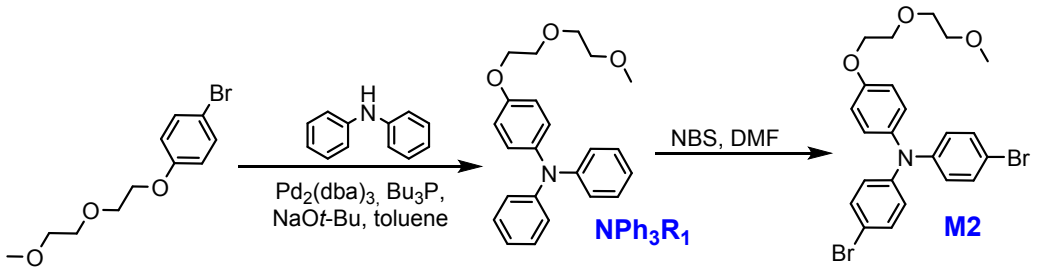

Figure S4. Synthesis of the ethylene glycol based triarylamine **M2**

Ethylene glycol based triarylamine $NPh_3R_1Br_2$ was synthesized using the same procedure as described above for 4-Bromo-*N*,*N*-bis(4-(2-(2-methoxyethoxy)ethoxy)phenyl)aniline [4,5] according to the **Figure S4**.

3. TGA measurements

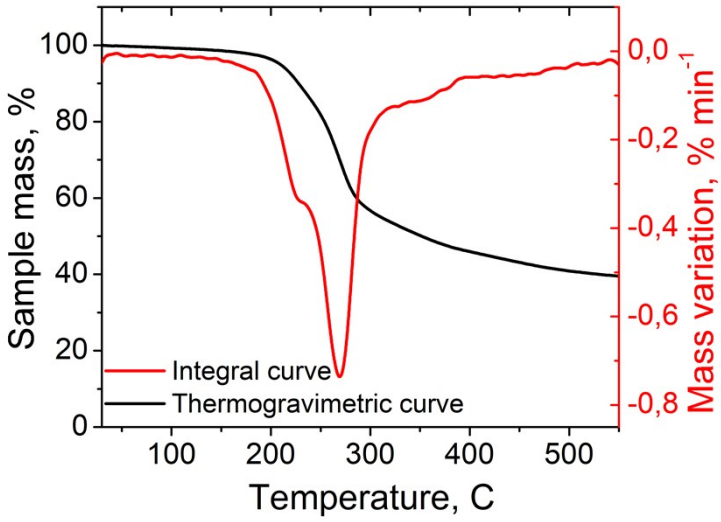

Figure S5. Thermal gravimetry curve of **M1**

4. *CV of the parent phenazine and M1 compound*

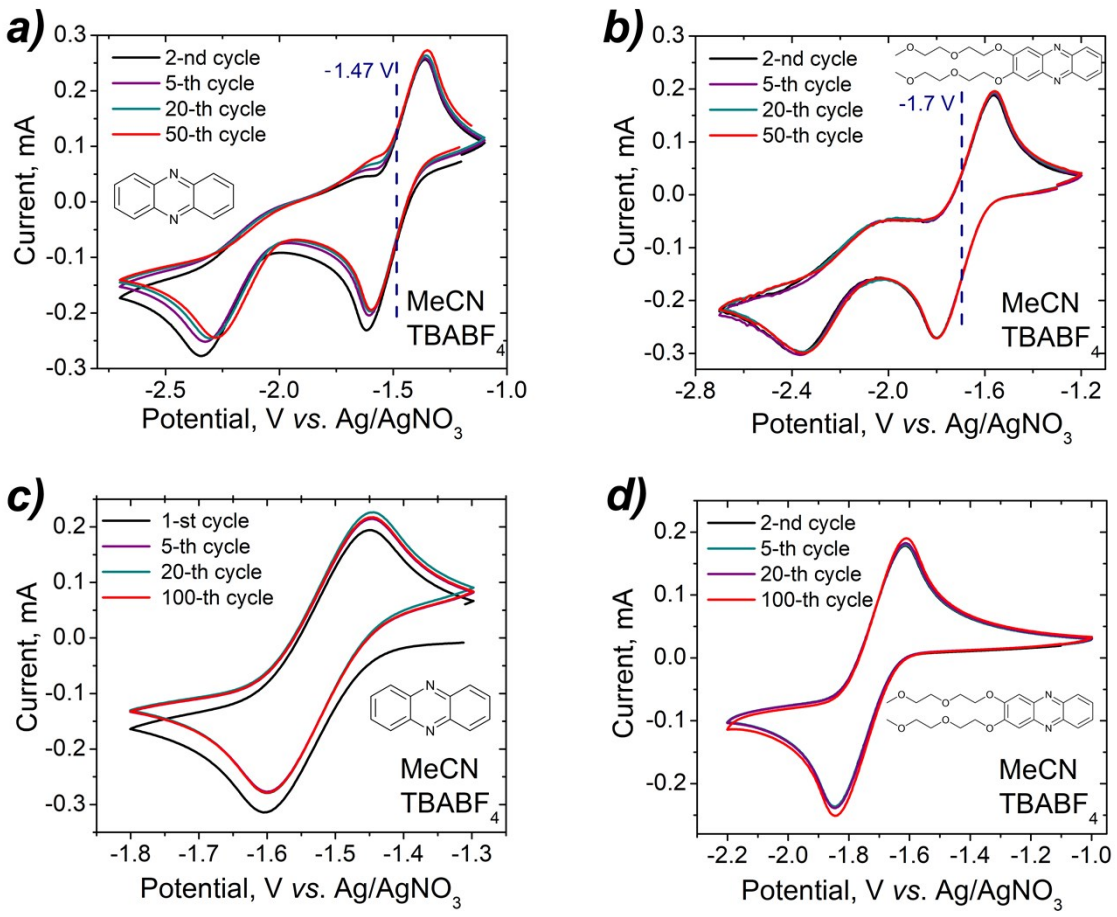

Figure S6. Cycling voltammograms obtained for 3.0 mM of **phenazine** (a, c) and **M1** compound (b, d) at low (c, d) and high (a, b) potential ranges with 0.1 M $TBABF_4$ MeCN as a supporting electrolyte.

5. Scan-rate-dependent CV measurements

The diffusion coefficient of **M1** was obtained by using the Randles-Sevcik equation for reversible systems:

$$i_{p,c} = 269\,000 \cdot n^{3/2} \cdot A \cdot D^{1/2} \cdot C \cdot \upsilon^{1/2}$$

where, $i_{p,c}$ is the peak current density in A; n is the number of transferred electrons; D is the diffusion coefficient in $cm^2\ s^{-1}$; A is the electrode area in cm^2; C is the concentration of the **M1** in mol cm^{-3}; υ is scan rate in V s^{-1}. [6]

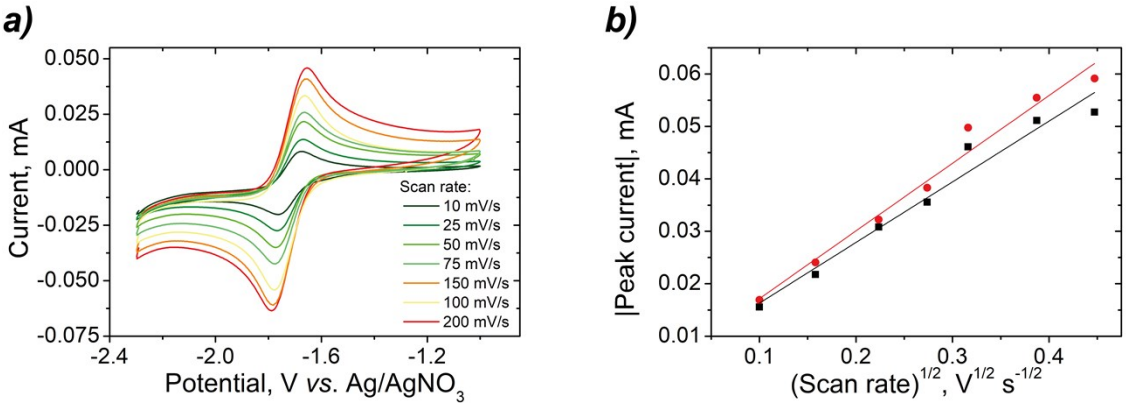

Figure S7. Scan-rate-dependent cycling voltammograms obtained for 3.0 mM MeCN solution of **M1** with 0.1 M $TBABF_4$ as a supporting electrolyte at different scan rates: (a) Current-voltage curves and (b) reduction and re-oxidation peak current versus square root of the scan rate.

Table S1. Scan rates, reduction and oxidation currents obtained for the scan-rate-dependent cycling voltammograms

Scan rate, mV s^{-1}	(Scan rate)$^{-1/2}$, $V^{1/2}\ s^{-1}$	Reduction peak current value (A)	Reduction peak current value after the ohmic drop compensation (A)	Oxidation peak current value (A)	Oxidation peak current value after the ohmic drop compensation in modulus (A)
200	0.4472	4.5741×10^{-5}	5.2730×10^{-5}	-6.3447×10^{-5}	5.9122×10^{-5}
150	0.3873	4.0728×10^{-5}	5.1131×10^{-5}	-6.0939×10^{-5}	5.5484×10^{-5}
100	0.3162	3.3669×10^{-5}	4.6100×10^{-5}	-5.4582×10^{-5}	4.9762×10^{-5}
75	0.2738	2.6001×10^{-5}	3.5557×10^{-5}	-4.2363×10^{-5}	3.8324×10^{-5}
50	0.2236	2.1867×10^{-5}	3.0810×10^{-5}	-3.5308×10^{-5}	3.2224×10^{-5}
25	0.1581	1.3771×10^{-5}	2.1761×10^{-5}	-2.7560×10^{-5}	2.4060×10^{-5}
10	0.1000	8.3004×10^{-6}	1.5579×10^{-5}	-2.0195×10^{-6}	1.6915×10^{-5}

The standard rate constant, k_0, was obtained by using the Nicolson method according to the equation:

$$k_0 = (\pi \cdot D \cdot f \cdot \upsilon)^{1/2} \cdot \Psi$$

where, k_0 is the standard rate constant in cm^{-1}; π is the mathematical constant; D is the diffusion coefficient; υ is scan rate in V s^{-1}; $f=(n \cdot F)/(R \cdot T)$; Ψ is the Nicolson dimensionless number. [7,8]

Table S2. Calculation of k_0 for the **M1**/**M1**$^{\bullet-}$ redox pair

Scan rate, mV s^{-1}	ΔE_p[a], mV	Ψ [b], (dimensionless)	$k_0 \times 10^{-3}$, cm s^{-1}	Average k_0, cm s^{-1}	Standard deviation, cm s^{-1}
200	131	0.29	0.003319	2.84×10^{-3}	4.87×10^{-4}
150	125	0.32	0.003171		
100	114	0.40	0.003237		
75	114	0.40	0.002803		
50	103	0.53	0.003033		
25	101	0.55	0.002225		
10	89	0.83	0.002124		

[a] ΔE_p: peak potential separation in CV curve.

[b] Ψ: Nicholson dimensionless number. The value was obtained from the Figure 3 and Table 1 in the Nicolson's paper. [7]

6. Flow cell resistance measurements

To estimate the potential drop of the RFB due to the IR losses, we performed impedance spectroscopy measurements for the complete cell and the cell without membrane. According to the impedance curves presented on Figure S8 the cell resistance could be estimated as ~180 Ω, the resistance of the cell without Neosepta AHA membrane ~70 Ω and the membrane resistance as ~110 Ω.

Therefore, we could conclude that the membrane gives the highest contribution to cell resistance. We assume that the replacement of the polymeric membrane to the porous separator could lead to the significant decrease of the cell resistance. The second component with a significant impact on the cell resistance is the Teflon/graphite current collectors, which were applied to prevent the acetonitrile leakage thought the graphite porous.

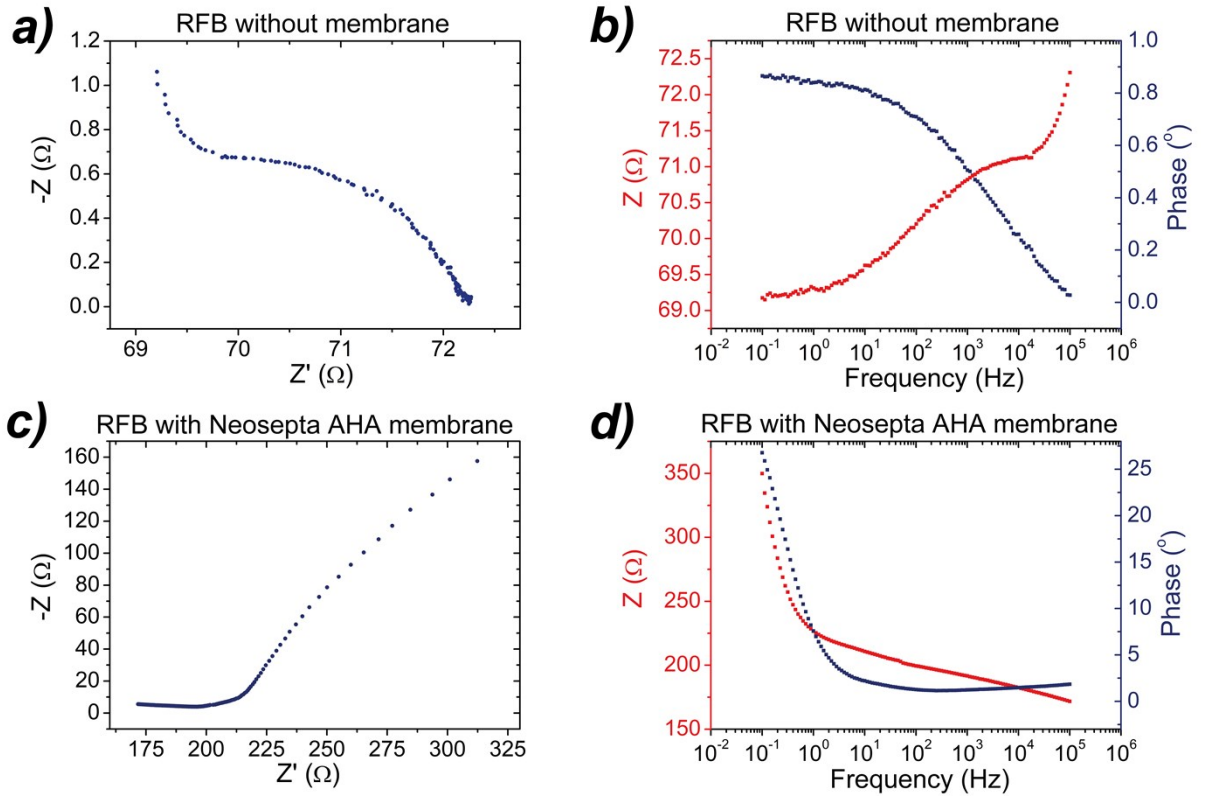

Figure S8. (a) The Nyquist Plot of the RFB cell without membrane; (b) The Bode Plot of the RFB cell without membrane; (c) The Nyquist Plot of the RFB cell with Neosepta AHA membrane; (d) The Bode Plot of the RFB cell with Neosepta AHA membrane.

7. References

1 Y. Kim, J. Choi, C. Lee, Y. Kim, C. Kim, T. L. Nguyen, B. Gautam, K. Gundogdu, H. Y. Woo and B. J. Kim, *Chem. Mater.*, 2018, **30**, 5663–5672.

2 C. Seillan, H. Brisset and O. Siri, *Org. Lett.*, 2008, **10**, 4013–4016.

3 J. Winsberg, C. Stolze, S. Muench, F. Liedl, M. D. Hager and U. S. Schubert, *ACS Energy Lett.*, 2016, **1**, 976–980.

4 H. Choi, J. Han, M. Kang, K. Song, J. Ko, *Bull. Korean Chem. Soc.,* 2014, **35**, 5б 1433–1439

5 E. Romadina, I. Volodin, K. Stevenson, P. Troshin, *JMC-A*, 2021, 10.1039/D0TA11860E

6 L. R. F. Allen J. Bard, *Electrochemical Methods: Fundamentals and Applications*, 2000.

7 R. Nicholson, *Anal. Chem*., 1965, **37**, 1351–1355.

8 K. Gong, Q. Fang, S. Gu, S. Li, Y. Yan, *Energy Environ. Sci.*, 2015,**8**, 3515–3530